

Strategic Incorporation of Cleavable Side Chains Improves Thermal Stability of PffBT-T4-Based Polymer Solar Cells

Published as part of Chemistry of Materials *virtual special issue* "In Honor of Prof. Elsa Reichmanis".

Jordan Shanahan, Jiyeon Oh, Sung Yun Son, Salma Siddika, David Pendleton, Brendan T. O'Connor, and Wei You*



Cite This: *Chem. Mater.* 2023, 35, 10139–10149



Read Online

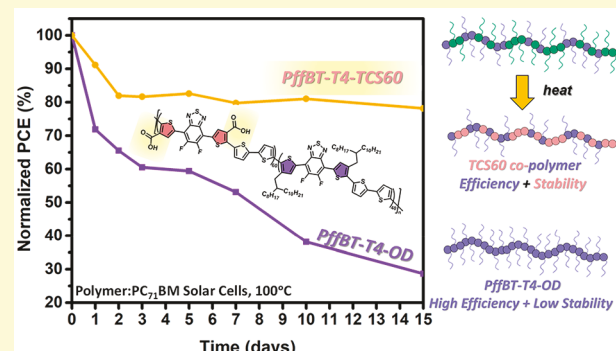
ACCESS |

Metrics & More

Article Recommendations

Supporting Information

ABSTRACT: Thermal degradation by intrinsic morphological change and extrinsic oxidation remain outstanding challenges for bulk heterojunction (BHJ)-based polymer solar cells (PSCs). Postprocessing thermocleavage of side chains on the donor conjugated polymers using ester pyrolysis is a proven method to kinetically trap the morphology via increased glass transition temperature (T_g) and improved thermal oxidation resistance. We previously showed that having a certain fraction of thermocleavable side chains (TCS) incorporated into the archetypical polymer P3HT, achieved through the copolymerization of a TCS-functionalized thiophene monomer, can offer high thermal stability to its BHJ devices without compromising significant performance metrics. This work expands the concept of using the copolymerized TCS monomer unit to balance the stability with efficiency into the state-of-the-art PSC system PffBT-T4-OD:PCBM, where the original octyl-decyl (OD) branched side chains are partially replaced with TCS in 50–70 mol % in the copolymers. Structural differences of the fully cleavable PffBT-T4-TCS polymer and P3ET polymers disclose that increasing backbone rigidity and alkyl chain length can increase the temperature of eliminating alkyl chains by up to 20 °C in the solid state. Dynamic mechanical analysis shows the cleaved PffBT-T4-TCS polymer has significantly increased thermal relaxation temperatures and high storage modulus over a large temperature range. Thermal stability testing at 100 °C in air reveals that increasing the TCS content drastically increases the polymer resistance to oxidation. PSCs made with the fully cleavable PffBT-T4-TCS polymer offer only a meager efficiency of 0.2%, while the copolymer with 60 mol % TCS can deliver a PCE of 3.2% with its BHJ device, double the previous highest reported efficiency for TCS-containing polymer-based PSCs. Importantly, the copolymer with the 60 mol % TCS-based device is stable, retaining 80% of the initial performance after accelerated aging tests (100 °C, 2 weeks). Together with our previous works, these new findings demonstrate that using partial cleavage of side chains could be a general strategy to gain both efficiency and stability for conjugated polymer-based PSCs.



INTRODUCTION

Bulk heterojunction (BHJ) polymer solar cells (PSCs) have made tremendous progress in the past three decades, with power conversion efficiencies (PCE) now approaching 20%.^{1–3} The development of “push–pull” conjugated polymers with low-lying highest occupied molecular orbital (HOMO) levels and narrow band gaps^{4,5} has skyrocketed PCEs to near 11%, benchmarked by the PffBT-T4-OD:fullerene system in 2014.⁶ The further innovation of non-fullerene acceptors with complementary light absorption to that of the donor polymer has pushed PCEs of binary PSCs above 19%.^{7,8} However, many of these champion BHJ blends rapidly degrade due to both intrinsic (e.g., light and heat) and extrinsic (e.g., water and oxygen) stressors.⁹ Significant efforts have been made on studying these degradation mechanisms in various

systems and are most often addressed on a case-by-case basis.^{9–12}

While a proper encapsulation of PSCs could largely mitigate the impact of external factors such as water and oxygen, addressing the intrinsic degradation by light and heat is much more challenging. For example, typically the optimized morphology of a BHJ blend is kinetically trapped in order to deliver the highest efficiency;¹² yet the multicomponent nature

Received: August 31, 2023

Revised: October 31, 2023

Accepted: November 1, 2023

Published: November 21, 2023



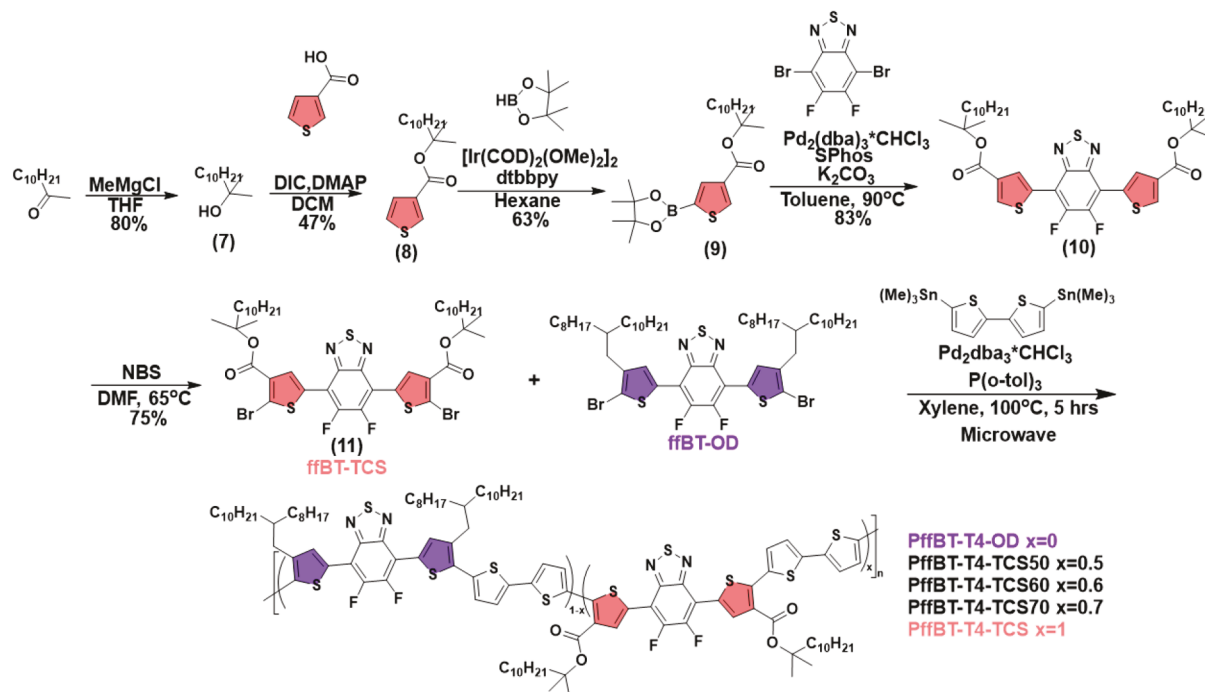
ACS Publications

© 2023 American Chemical Society

10139

<https://doi.org/10.1021/acs.chemmater.3c02181>
Chem. Mater. 2023, 35, 10139–10149

Scheme 1. : Synthesis of PffBT-T4-TCS Polymer and Copolymers



of the BHJ blend is thermodynamically unstable and would deteriorate upon high temperature, resulting in significantly diminished device efficiency. Materials with high glass transition temperatures (T_g) can largely withstand heat-induced morphological change, yet most conjugated polymers do not demonstrate sufficiently high T_g (e.g., over $100\text{ }^\circ\text{C}$) because “low- T_g ” alkyl chains (often over 50 wt % of the conjugated polymer) are required to impart the solubility of conjugated polymers in processing solvents.^{13–15} To improve the T_g of the conjugated polymer in the finished BHJ device and thereby the device stability, thermally removing these alkyl chains via tertiary ester-based pyrolysis had been developed.^{16,17} Cleavable side chains have been frequently used in different types of organic electronic devices (including PSCs, transistors,^{18–20} and chemical sensors^{21,22}) with a variety of cleavable chemistries.^{23–26} However, when used in PSCs, only low PCE numbers (typically less than 1%) were obtained, albeit the BHJ film/device was indeed much more stable after removing alkyl chains.¹⁷ Recognizing that removing *all* alkyl chains could have a strong (negative) impact on the morphology of the BHJ blend, we recently designed a strategy to minimize the impact of thermocleavage to the BHJ morphology, yet still enjoy the benefits of removing alkyl chains toward device stability.²⁷ Using P3HT:PCBM as the model system, we explored a series of polythiophenes with different molar ratios of a thiophene unit bearing the tertiary ester containing a thermocleavable alkyl chain (TCS) (i.e., ET) and the original 3-hexylthiophene monomer (HT). While the 100% TCS-containing polymer (i.e., P3ET) was likely the most stable (after thermocleavage of alkyl chains), its BHJ device gave only negligible efficiency. On the other hand, the TCS60 polymer, which contains 60 mol % TCS and 40 mol % original hexyl chains, demonstrated the highest efficiency ($\sim 1.3\%$) and excellent stability at $150\text{ }^\circ\text{C}$ over a long period of time. Mechanistically, it was proposed that retaining a certain fraction of the alkyl chains (hexyl in this case) could help

maintain the desirable morphology for high efficiency, yet removing the rest of the alkyl chains would raise the T_g of the polymer and kinetically vitrify the morphology for better stability.^{12,27,28} Additionally, the carboxylic acid functional group remaining on the thiophene unit after elimination of the TCSs can provide resistance to thermal oxidation observed in conjugated polymer films by lowering the oxidation potential of the conjugated polymer and elimination of low-energy degradation pathways initiated on alkyl chains.^{29–32}

However, P3HT represents the earlier examples of conjugated polymers for PSCs; state-of-the-art conjugated polymers that can achieve high PCEs in BHJ cells are typically “push–pull” polymers that were synthesized by polycondensation. Applying the strategy of cleavable alkyl chains to such “push–pull” polymers has been rarely reported, and only modest PCEs (<2%) were obtained.^{16,22,33–36} Given the success of using partial cleavage of alkyl chains in our previous study on P3HT/P3ET, we set our goal to apply the same strategy to the state-of-the-art “push–pull” polymers and to explore its potential in achieving stable PSCs without sacrificing significant PCE.

The PffBT-T4-OD:PCBM system demonstrates the apex of PCE achieved for a polymer:fullerene-based PSC, where the optimized ethyl-2-octyl-decyl (OD) side chains are crucial to the temperature-dependent aggregation behavior, leading to an optimized BHJ morphology.^{6,37} However, this system also suffers from severe morphological burn-in degradation where up to 32% of the initial device efficiency was lost within 5 days in inert room temperature conditions.^{38,39} Thus, this system was chosen to test our TCS copolymerization strategy where a portion of the original OD alkyl chains would be directly replaced by the TCS units in a systematic manner (i.e., 25–70 mol % TCS in the finished copolymers). Thermogravimetry analysis (TGA) characterization revealed that the PffBT-T4-TCS polymer (i.e., 100 mol % TCS), incorporating the same tertiary 3-ester thiophene functionality in our earlier work, had

a 20 °C higher onset temperature (T_c) and slower cleavage rate than the polythiophene with 100 mol % TCS (i.e., P3ET) in our earlier study. This difference was ascribed to a kinetic effect of the stiffer polymer backbone. Evaluating all polymers individually in BHJ solar cells showed that 60% TCS incorporation (i.e., PffBT-T4-TCS60) maintains a moderate efficiency of 3.2% (after thermocleavage) but leads to an intrinsically stable morphology (BHJ blend) than the original PffBT-T4-OD. Pleasingly, TCS60 polymer-based devices showed a retention of 80% of the initial PCE after 2 weeks at 100 °C, while the PffBT-T4-OD-based device lost over 70% of its original PCE.

■ SYNTHESIS AND INITIAL CHARACTERIZATION OF PffBT-T4 SERIES POLYMERS

Scheme 1 outlines the chemical structures and synthetic routes of the TCS series PffBT-T4-based polymers. The monomer, ffbT-TCS (11), was synthesized via the bromination of the product from Suzuki coupling of the TCS-based thiophene–boronic ester unit (9) and the electron-deficient 5,6-difluorobenzothiodiazole–dibromo unit. Details of the synthetic procedures and relevant characterizations of all compounds are listed in the *Supporting Information*. Different molar ratios of the commercial “high-efficiency” monomer ffbT-OD vs ffbT-TCS monomer were employed to prepare the targeted series of PffBT-T4-TCS x copolymers through Stille step growth polycondensation with bis-stannylated bithiophene as the other comonomer. Note that the series of TCS-based copolymers are designated as PffBT-T4-TCS x ($x = 50, 60, \text{ and } 70$) and PffBT-T4-TCS ($x = 100$), where x denotes the molar ratio of the ffbT-TCS monomer.

Initially, a shorter alkyl-based TCS, 2-methylhexyl side chains (C4), was used for this series of PffBT-T4-TCS x . Unfortunately, only insoluble polymer was produced when using ffbT-TCS (C4), and only PffBT-T4-TCS25 was confirmed to be soluble in hot chlorobenzene (**Figure S1**). Therefore, the length of the alkyl chain was extended to C10 to improve solubility, allowing the synthesis of copolymers (PffBT-T4-TCS x and PffBT-T4-TCS) containing 50% or higher TCS content. The original PffBT-T4-OD polymer was also synthesized as the control. As expected, the longer side chains provided necessary solubility to the copolymers as well as the PffBT-T4-TCS homopolymer. Specifically, the PffBT-T4-OD and all PffBT-T4-TCS x copolymers were found to be only soluble in hot chlorobenzene up to 12 mg/mL. By contrast, 84% of the PffBT-T4-TCS homopolymer was able to be extracted in the chloroform fraction from the Soxhlet extraction leaving behind no residue. The PffBT-T4-TCS homopolymer exhibited partial solubility (<1 mg/mL) in Tetrahydrofuran (THF) and 2-methyl-THF and 20 mg/mL solubility in chloroform, toluene, and *o*-xylene. We attribute this greater solubility of the PffBT-T4-TCS homopolymer to the polar ester unit and the bulky tertiary ester side chains which would inhibit extensive aggregation behavior.

The molecular weights and dispersities of all polymers are summarized in **Table 1**. As shown in **Figures S2–S8**, the true molar ratios of TCS monomer in the polymer backbone were verified by ^1H nuclear magnetic resonance (NMR) spectroscopy, which are in good agreement with the feed ratios (within a 5% mismatch). Moreover, TGA also quantitatively confirms the weight ratios of TCS in the polymer (**Figure 1**) with expected weight losses near 220 °C T_c , confirming ester pyrolysis and evaporation of cleaved alkyl chains. Measured

Table 1. Polymer Synthesis, Characterization, and Thermal Degradation

PffBT-T4 polymer ^a	TCS in synthesis (mol %)	TCS in polymer ^b (mol %)	M_n (to D) ^c [kg/mol]	T_c [°C] ^d	wt % loss after T_c (Th) ^e
TCS100	100	100	18.8 (1.7)	219.2	30.6 (38.3)
TC570	70	68.9	47.4 (1.8)	221.4	25.9 (26.4)
TC560	60	62.5	18.0 (2.1)	222.9	22.1 (22.0)
TC550	50	54.1	19.3 (1.8)	222.8	18.1 (18.4)
TC525	25	18.5	N/A	228.7	6.6 (7.18)
OD	0	0	35.9 (1.4)		N/A

^aAll polymers were made with 2-methylundecyl side chains (C10). TCS25 was made using 2-methylhexyl chains (C4) and MW could not be obtained by GPC due to solubility issue. ^bMol % was calculated using ^1H NMR spectra. ^cMolecular weight measured using HT-GPC at 90 °C in trichlorobenzene, against a polystyrene standard curve. ^dThermal cleavage onset temperatures extracted from TGA using tangent fitting. ^eWt % loss was measured after the first weight loss transition correlating with total elimination of alkene taken at 270 °C in each TGA scan.

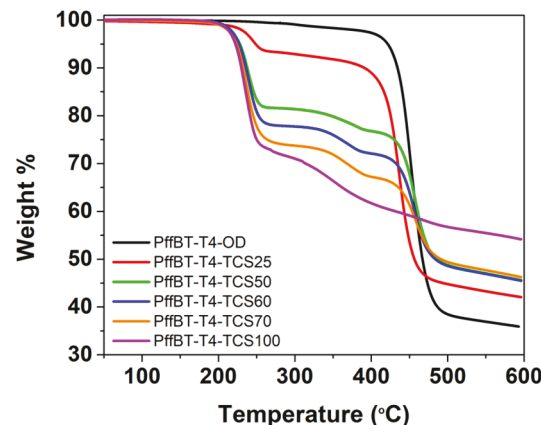


Figure 1. TGA of all polymers synthesized in this study taken at a 10 °C/min scan rate.

mass losses matched well with theoretically calculated losses within 5 wt % for all copolymers and 9 wt % for the TCS containing homopolymer. All TCS-containing copolymers exhibit three distinct weight loss transitions near 220, 300, and 450 °C, coinciding with alkene elimination, decarboxylation, and alkyl decomposition of the ffbT-OD unit, respectively. Mechanisms for elimination of the thermocleavable alkyl chains and decarboxylation are provided in **Scheme S3** and were discussed in our previous work.²⁷ All PffBT-T4-TCS x polymers became completely insoluble in all common processing solvents after the elimination of thermocleavable alky chains. Although decarboxylation occurs before the catastrophic decomposition step for all copolymers, temperatures >300 °C are not ideal for current device fabrication procedures and were not applied in this study.

Ultraviolet–visible (UV–vis) absorption spectroscopy was next conducted to assess the optical properties of all polymers in chlorobenzene solution and the corresponding thin-film states. Strong temperature-dependent aggregation in solution is an important property of the original OD-based polymer.⁶ Indeed, the PffBT-T4-OD shows significant signs of disaggregation with increasing temperature (**Figure 2a**), and a transition between ordered and disordered structure near 90 °C was observed where the relative intensities of the 0–0 and

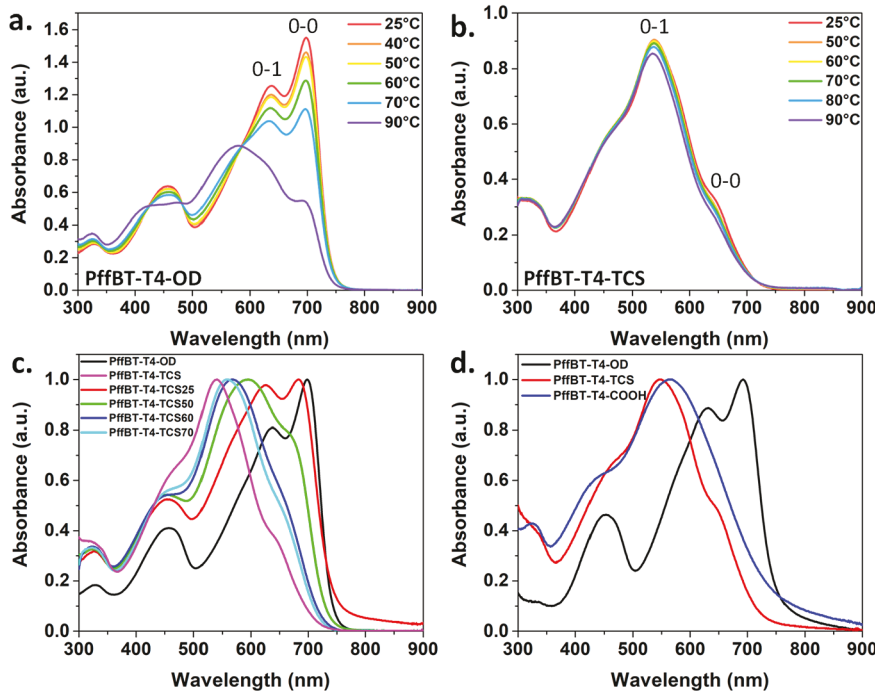


Figure 2. (a) Temperature-dependent UV/vis absorption of PffBT-T4-OD at 0.02 mg/mL in chlorobenzene. (b) Temperature-dependent UV/vis absorption of PffBT-T4-TCS polymer at 0.02 mg/mL in chlorobenzene. (c) UV/vis of all polymers at 0.02 mg/mL in chlorobenzene. (d) UV/vis of as-cast TCS and OD films and the TCS film (COOH polymer) after annealing at 220 °C for 30 min.

0–1 vibrational peaks switch. PffBT-T4-TCS (i.e., TCS 100) containing bulky TCS units exhibits much less pronounced changes in absorption spectra with temperature, as there is only a slight loss in absorption intensity when temperature is raised past 90 °C (Figure 2b). This behavior can be ascribed to the steric hindrance from these bulky TCS units that prevents the aggregation of the TCS polymers. Moreover, with increasing fFBT-TCS monomer content in the polymer backbone, the resulting copolymers produce less temperature-dependent aggregation behavior (Figure S11), but they also retain greater relative intensity of the 0–0 peak in both solution and films. Overall, this qualitative analysis exemplifies that despite having identical conjugated backbone, the steric hindrance of TCSs largely mitigates desirable aggregation behavior, which could lead to poorer performing devices (*vide infra*).

The fact that the steric hindrance of the TCS units prevents the aggregation of conjugated polymers could also explain the significant blue-shift in the case of PffBT-T4-TCS compared to PffBT-T4-OD in thin films and solution (Figures 2c and 2d). On the other hand, the ester group of the TCS unit on the conjugated backbone apparently exerts a stronger impact (than the steric hindrance) on the measured HOMO energy level: the estimated HOMO level of the PffBT-T4-OD (−5.42 eV) via cyclic voltammetry is noticeably lower than that of PffBT-T4-TCS (−5.24 eV) (Table 2 and Figure S10); this interesting observation is tentatively ascribed to the subtle electronic effect of the ester group on the overall “donor–acceptor” nature of PffBT-T4-TCS.

■ EFFECTS OF CHEMICAL STRUCTURE ON THERMAL CLEAVAGE

To explore the structural effects on the thermal cleavage of side chains, three TCS-homopolymers were thoroughly examined:

Table 2. Optoelectronic Properties Comparison of TCS and OD Homopolymers

polymer	E_{OX} (V)	HOMO (eV)	E_{RED} (V)	LUMO (eV)	E_{g}^{CV} (eV)	$E_{\text{g}}^{\text{Opt}}$ (eV)
PffBT-T4-TCS	0.53	−5.24	−1.67	−3.04	2.20	1.71
PffBT-T4-OD	0.71	−5.42	N/A	−3.78 ^a		1.64

^aLUMO (lowest unoccupied molecular orbital) energy level is estimated from the HOMO energy level and $E_{\text{g}}^{\text{Opt}}$

P3ET-C4 (the original P3ET), P3ET-C10, and PffBT-T4-TCS (Figure 3a). Comparing P3ET (C4) and P3ET-C10 would disclose the effect of side-chain length on the thermocleavage, including thermal cleavage rate, onset temperature, and activation energy. On the other hand, comparing P3ET-C10 and PffBT-T4-TCS would show the effect of backbone structure on thermocleavage. In addition, the monomer and dimer units (Figure S14) were also investigated to understand whether macromolecules would have any impact on thermocleavage. Because the thiophene unit is the most commonly employed heteroaromatic unit in conjugated polymers for PSCs, we hope to use this section as a foundation for further exploration of TCS in the field.

As shown in Table 3 and Figure 3, the thermal cleavage onset temperature and inflection temperature for P3ET-C10 are approximately 10 °C higher than those for P3ET-C4. However, the activation energies extracted using the Flynn–Wall–Ozawa isoconversional method⁴⁰ show negligible difference between these polymers (details in the *Supporting Information*). Because both polymers share the identical backbone, this small change in onset difference between polymers can be explained by the difference in boiling point/vapor pressure of the side chain: eliminated C4-based alkenes boil between 90 and 95 °C while eliminated C10-based alkenes boil between 225 and 230 °C. While the lower volatility of

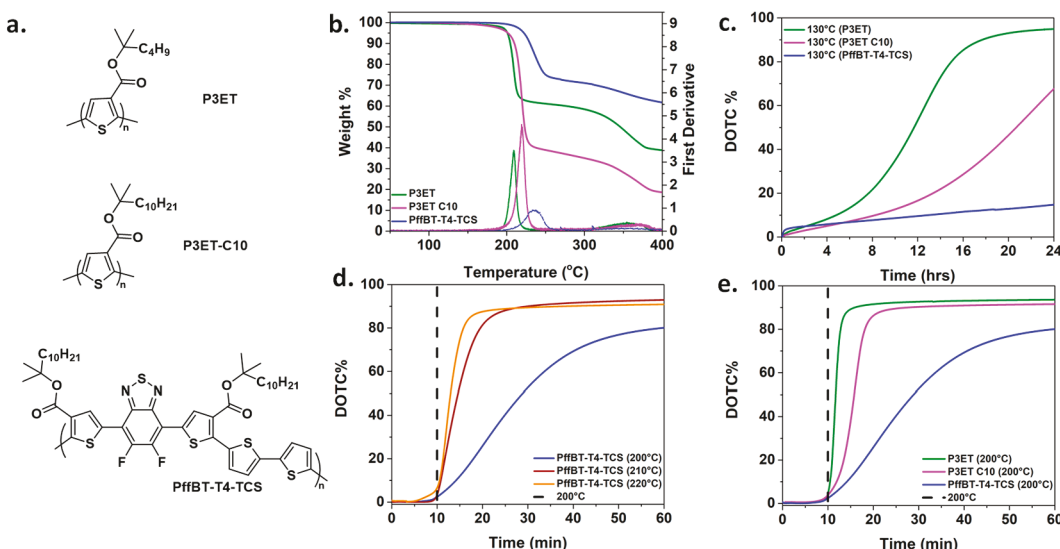


Figure 3. (a) Chemical structures of polymers used for cleavage rate study. (b) TGA data and first-derivative TGA data of TCS homopolymers used for rate study at a 10 °C/min scan rate. (c) Isothermal annealing of TCS polymers at 130 °C for 24 h. (d) Isothermal annealing of PffBT-T4-TCS at 200, 210, and 220 °C for 60 min. The dashed line is when the TGA reaches 200 °C. (e) Isothermal annealing of TCS polymers at 200 °C for 60 min. The dashed line is when TGA reaches 200 °C.

Table 3. TGA Analysis of Side Chain Cleavage

polymer	activation energy (SD) [kJ/mol] ^a	T_c ^b [°C]	inflection temperature [°C] ^c
P3ET	113.5 (2.5)	201.3	208.4
P3ET (C10)	110.0 (6.6)	210.6	218.8
PffBT-T4-TCS	117.5 (5.9) ^d	219.2	234.7

^aActivation energies calculated using the Ozawa method (Supporting Information) from different TGA heating rates. ^bThermal cleavage onset temperatures extracted from 10 °C/min TGA curves. ^cInflection temperature calculated from first derivative of 10 °C/min TGA curves. ^dActivation energy estimated from the TCS70 polymer.

C10-based alkene decreases the rate of thermal cleavage slightly, according to TGA experiments and isothermal annealing at 200 °C (Figures 3a and 3b), a much larger difference in the rate of cleavage between the two side chains appears at the low-temperature cleavage limit of 130 °C, where P3ET-C4 cleaved to within 95% in 24 h and P3ET-C10 only cleaved to 75% (Figure 3c).

On the other hand, both thermocleavage onset temperature and the inflection temperature for the “push–pull” polymer PffBT-T4-TCS are appreciably higher than those of P3ET-C10 which has the identical TCS (Table 3), indicating that the polymer backbone structure also has a strong impact on thermal cleavage rate. While the onset cleavage temperature is only a further 8 °C higher for PffBT-T4-TCS than P3ET-C10, the inflection point of PffBT-T4-TCS cleavage occurs an unexpected 24 °C higher temperature. Isothermal analysis at 130 °C (Figure 3c) discloses that only 10% of PffBT-T4-TCS side chains were cleaved in 24 h. Furthermore, at the 200 °C temperature we used in previous reports for rapid thermal cleavage (Figure 3e), both P3ET-C4 and P3ET-C10 exhibit >90% DOTC (degree of thermocleavage) within the arbitrary 10 min time frame while PffBT-T4-TCS requires over 1 h to cleave 80% of its side chains. Data from applying different annealing temperatures of PffBT-T4-TCS (Figure 3d) indicate that 220 °C was needed to cleave over 90% of side chains

within 10 min, and this temperature was therefore used for fabricating BHJ devices and thin films tested in this work. Further Fourier-transform infrared spectroscopy (FT-IR) experiments (Figure S13) of PffBT-T4-TCS films complement the TGA experiment well, where the carbonyl CO stretch at 1708 cm⁻¹ is shifted to 1716 cm⁻¹ and broadened after annealing at 220 °C for 30 min, indicating the transition from the ester (precleavage of alkyl chains) to carboxylic acid (after thermocleavage). The disappearance of the CH stretching at 2925 cm⁻¹ and the appearance of broad OH stretching from 3400 to 3500 cm⁻¹ are also observed, supporting the formation of carboxylic acid (COOH). Furthermore, spun-cast films of the PffBT-T4-TCSx copolymers (100–150 nm) showed thickness reduction after the annealing step, matching the expected mass loss well (Table S1). No change in the FT-IR spectrum or thickness compared to the as-cast film was observed after heating at 150 °C for 24 h, indicating a minimum amount of cleavage (if any). However, when dissolving PffBT-T4-TCS in 1,2-dichlorobenzene-*d*₂ (NMR solvent) and heating the solution at 140 °C for 14 h, the elimination of two isomers of alkene was confirmed by ¹H NMR spectroscopy, together with precipitated polymer (Figure S9). This observation demonstrates that homogeneously dispersing polymers in good solvents can facilitate thermocleavage.

To account for the significant differences in the cleavage rate between PffBT-T4-TCS and P3ET-C10, we considered two plausible explanations. First, the electronic structure of the polymer can lower the enthalpy for elimination. The tertiary ester syn-elimination reaction proceeds through a concerted E1 mechanism with a six-membered transition state.^{41,42} Previous reports on TCS have demonstrated that functional groups next to the tertiary carbon can lower the energy of this transition state and lower the temperature of cleavage.^{43,44} Because all three polymers tested (in this study) have the same functionality (i.e., thiophene) attached to the tertiary ester and there is no difference in measured activation energy, there should be no significant differences resulting from the electronic effect. The second possibility is that PffBT-T4-

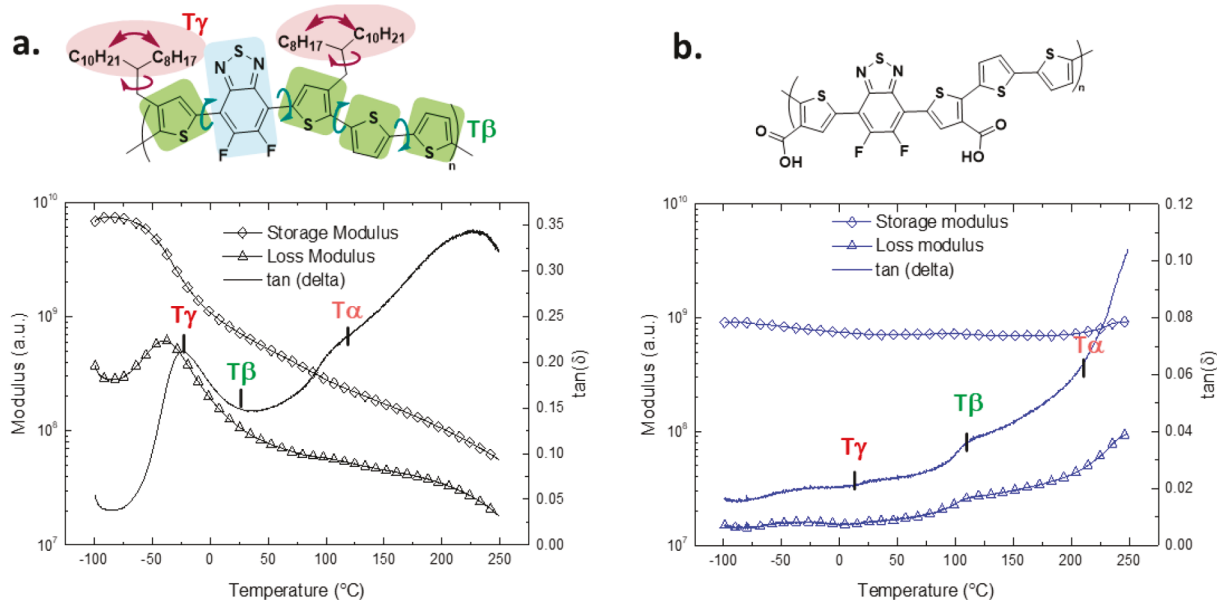


Figure 4. (a) DMA graph of PffBT-T4-OD, including thermal relaxation temperatures and chemical structure with attributed relaxations. (b) DMA graph of cleaved PffBT-T4-COOH (PffBT-T4-TCS polymer after thermocleavage) and its chemical structure.

TCS's entropy of elimination is lower due to its higher rigidity of the polymer in the solid state than P3ET-C10. PffBT-T4-OD (the TCS-free analogue) has a very rigid backbone (persistence length = 3.7 nm) compared to P3HT (persistence length = 2.7 nm).¹³ Substituting the OD or hexyl side chains with TCS would introduce the steric hindrance (from TCS) to the conjugated backbone and reduce the chain rigidity, which would lead to a lower temperature of thermocleavage. Indeed, experimental data show that increasing density of TCS on the PffBT-T4 copolymer decreases the onset temperature of cleavage (Table 1), with lowest temperature observed for PffBT-T4-TCS (i.e., 100% TCS). In fact, similar behavior was also observed for the P3ET/P3HT copolymers, where P3ET-C4 (i.e., 100% TCS) showed the lowest temperature of cleavage.²⁷

Because of the complexities of measuring polymer rigidity (which will be discussed later in this work), we are not able to construct a numerical correlation between a material value (e.g., glass transition) and cleavage rate. We instead chose to indirectly test this hypothesis with two dimers (and also structural isomers) of ET, OET, and IET, together with the “monomer” of PffBT-T4-TCS, ffBT (C4). OET is a crystalline powder with esters on the 4 positions (outside positions), and IET is an amorphous oil with esters on the 3 positions (inside positions) at room temperature (structures shown in Figure S14). TGA data show that the more crystalline/rigid ffBT monomer and OET dimer has a 20 °C higher cleavage temperature than the amorphous IET dimer (Figure S15), consistent with the observed higher cleavage temperature of PffBT-T4-TCS than P3ET-C10. Additionally, the ffBT-TCS monomer also has a lower cleavage temperature than the PffBT-T4-TCS polymer, implying that the macromolecular structure could increase the cleavage temperature. Overall, our brief study suggests that rigidity of backbone in conjugated polymers impacts the rate of thermal cleavage more significantly than the length of the alkyl chain on the TCS unit.

■ THERMOMECHANICAL PROPERTIES RELATING TO INTRINSIC STABILITY

Characterization of all polymers with differential scanning calorimetry (DSC) (Figure S16) did not reveal clear glass transition for any PffBT polymer; however, PffBT-T4-OD has a reversible melting peak at 262 °C, while PffBT-T4-TCS has no observable melting peak and a large endothermic transition around 220 °C, coinciding with thermal cleavage of side chains. The first cooling scan and second heating scan in the range of -10 to 300 °C of PffBT-T4-TCS did not show any other thermal transition, indicating the vitrification of the polymer. The copolymers TCS50, TCS60, and TCS70 have similar thermal behavior, with lower enthalpies of thermal elimination for the cleavage step with lower TCS content.

The vitrification of the polymer is better exemplified using dynamic mechanical analysis (DMA) (Figures 4 and S17), which is more sensitive at detecting thermal relaxation in conjugated polymers than DSC alone. In typical commodity polymers, the T_g is taken as the metric for identifying the transition between a viscous liquid and frozen glass in the amorphous phase of the polymer. Most push–pull conjugated polymers, however, possess no clear glass transition due to their comb-like structures and high crystallinity.^{14,15,45} Instead, most such polymers possess localized mechanical relaxations along the side chain (T_γ), backbone (T_β), and rigid amorphous phase (T_α), often with side-chain relaxation being the dominating feature and occurring at temperatures below 0 °C. The temperatures of these transitions are extracted from Gaussian fitting the $\tan(\delta)$ (Figures S18–S20) as in previous reports.¹⁵

PffBT-T4-OD and PffBT-T4-TCS show pronounced peaks in $\tan(\delta)$, coinciding with thermomechanical relaxations of the side chain and backbone and a decreasing storage modulus with increasing temperature. For PffBT-T4-OD, three distinct transitions occur in the $\tan(\delta)$ at -28, 4.9, and 106 °C, which are assigned as T_γ , T_β , and T_α , respectively. The corresponding temperatures for PffBT-T4-TCS are 49.4, 19.4, and 89.6 °C, respectively. Given that the side chain is 54% of the total

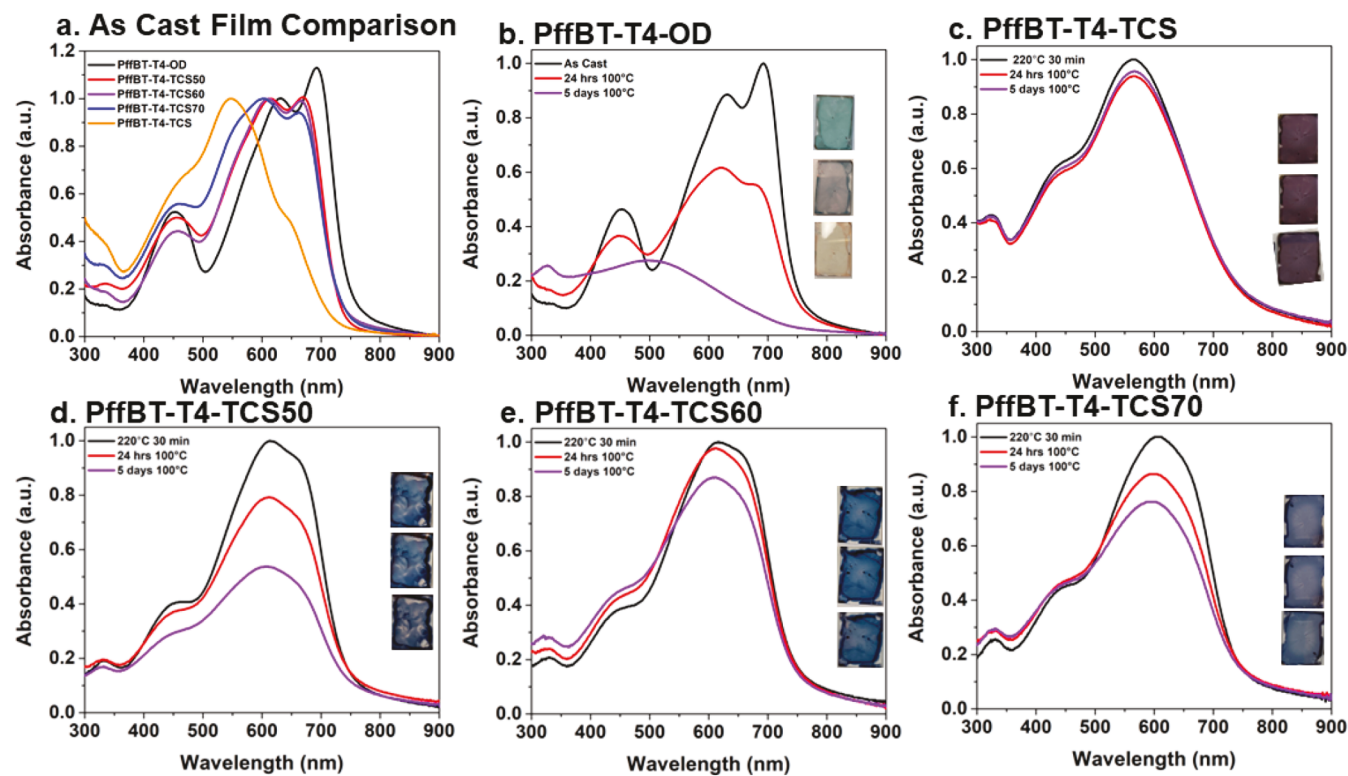


Figure 5. (a) As-cast polymer films (spun-cast at 10 mg/mL in chlorobenzene at 600 rpm). The PffBT-T4-TCS polymer was spun-cast at 20 mg/mL for similar thickness. UV/vis of polymer films after annealing at 220 °C for 30 min, followed by at 100 °C for 24 h, and last by at 100 °C for 5 days. Photos of films are shown after each annealing step in order from top to bottom.

weight of PffBT-T4-OD, the T_g is the most pronounced transition with a steep loss in storage modulus and sharp peak in $\tan(\delta)$ (Figure 4a). On the other hand, once PffBT-T4-TCS was heated to 220 °C for 30 min (to thermally remove alkyl chains), as-formed PffBT-T4-COOH shows a more consistent storage modulus with temperature and a smaller loss modulus and $\tan(\delta)$ than PffBT-T4-TCS or PffBT-T4-OD. The first three thermal relaxations for PffBT-T4-COOH are fitted as 10.6, 115.6, and 209 °C, further demonstrating a significant enhancement of thermomechanical properties compared to the other two polymers.

■ EXTRINSIC THERMAL STABILITY OF NEAT POLYMER FILMS

Our previous works have shown that, upon thermally removing the alkyl chains, the pendent carboxylic acid groups in cleaved TCS polymers help reduce oxidation potentials and increase resistance of the vitrified polymer films to external stressors (e.g., oxygen and water).^{27,29} In addition to lower oxidation potentials, eliminating alkyl chains removes radical-based hydrogen abstraction which can serve as a pathway for further degradation of the conjugated polymer (Scheme S4).^{29,32} To evaluate the stability of this series of polymers, neat polymer films (after thermocleavage) were first studied using UV/vis absorption spectroscopy in air (40–50 nm films, relative humidity ~57%, 100 °C in the dark for 5 days). Prior to thermocleavage, the two reference polymers (PffBT-T4-OD and PffBT-T4-TCS) show similar absorption profiles in their thin films (Figure 5a) to those in their solutions (Figure 2c); however, the three copolymers (TCS50, -60, and -70) clearly show more aggregation in the solid state when compared with their solution state. This observation indicates that retaining a

certain fraction of the strong aggregation polymer (i.e., PffBT-T4-OD) can preserve the strong interaction/aggregation even in copolymers, which could be beneficial to BHJ devices. On the other hand, the as-cast PffBT-T4-OD polymer film is the least stable among this series of polymers, losing 40% of its initial absorption in 24 h under 100 °C annealing (Figure 5b). Additionally, the relative heights of the 0–1 and 0–0 absorption peaks flip, and the band edge blue-shifts, indicating that a more amorphous morphology becomes dominant. After 5 days under 100 °C, the film was completely bleached (losing 72% of the initial absorption), and the spectrum is entirely blue-shifted with no aggregation-related peaks. In complete contrast, the PffBT-T4-COOH polymer (PffBT-T4-TCS after thermocleavage) retains 95% of its initial absorption after 5 days under 100 °C with no change in spectral shape (Figure 5c). Other copolymers show the expected trend of higher absorption retention with greater TCS content (Figures 5d–f). Specifically, the TCS50 copolymer shows a loss of 20% of its initial absorption after 1 day and a loss of 50% of its initial absorption after 5 days with a higher retention of spectral shape and smaller blue-shift than PffBT-T4-OD. On the other hand, the TCS60 copolymer shows much higher stability: retaining 98% of the initial absorption after 1 day and 80% by day 5. Interestingly, the TCS70 copolymer demonstrates slightly lower absorption retention than TCS60, 90% and 75% after 1 and 5 days, respectively; yet, the longer term stability of TCS60 and TCS70 is comparable (e.g., after 5 days). These data indicate that applying the TCS strategy to more contemporary “push–pull” conjugated polymer is also effective to significantly improve the stability of such polymers (after thermocleavage of alkyl chains on TCS) in air.

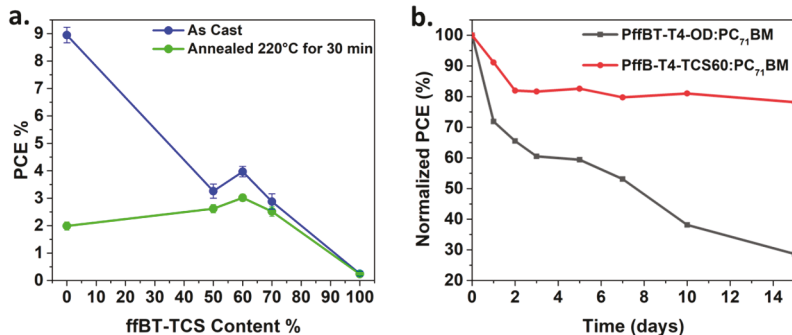


Figure 6. (a) Average PCE vs TCS content for polymer:PC₇₁BM solar cells before and after thermal annealing at 220 °C for 30 min. (b) Solar cell stability study for TCS60 and the reference polymer in BHJ solar cells at 100 °C in an inert atmosphere (i.e., nitrogen-filled glovebox) and under darkness. The cell efficiency was normalized vs time.

Table 4. Photovoltaic Performance of PffBT-T4-TCS_x:PC₇₁BM PSCs as Cast and Annealed at 220 °C for 30 min

system	V_{oc}^a [V]	J_{sc}^a [mA cm^{-2}]	FF ^a [%]	PCE ^a [%]
PffBT-T4-OD (as cast)	0.715 (0.713 ± 0.001)	18.34 (18.01 ± 0.30)	69.94 (69.77 ± 0.28)	9.17 (8.95 ± 0.28)
PffBT-T4-OD (220 °C)	0.576 (0.570 ± 0.002)	6.06 (5.85 ± 0.31)	60.34 (59.86 ± 0.32)	2.10 (1.99 ± 0.15)
PffBT-T4-TCS50 (as cast)	0.575 (0.570 ± 0.003)	14.30 (13.92 ± 0.54)	41.47 (41.07 ± 0.13)	3.41 (3.26 ± 0.26)
PffBT-T4-TCS50 (220 °C)	0.716 (0.716 ± 0.001)	7.64 (7.34 ± 0.45)	50.21 (49.82 ± 0.22)	2.75 (2.62 ± 0.15)
PffBT-T4-TCS60 (as cast)	0.605 (0.601 ± 0.005)	14.74 (14.41 ± 0.32)	46.47 (45.82 ± 0.28)	4.14 (3.97 ± 0.19)
PffBT-T4-TCS60 (220 °C)	0.761 (0.758 ± 0.002)	8.05 (7.90 ± 0.18)	51.50 (50.56 ± 0.48)	3.16 (3.02 ± 0.13)
PffBT-T4-TCS70 (as cast)	0.600 (0.600 ± 0.002)	11.99 (11.62 ± 0.46)	42.17 (41.38 ± 0.36)	3.03 (2.88 ± 0.28)
PffBT-T4-TCS70 (220 °C)	0.749 (0.739 ± 0.001)	7.30 (7.07 ± 0.33)	49.68 (48.31 ± 0.57)	2.71 (2.52 ± 0.18)
PffBT-T4-TCS (as cast)	0.378 (0.374 ± 0.003)	2.13 (1.86 ± 0.22)	35.63 (35.33 ± 0.12)	0.29 (0.25 ± 0.09)
PffBT-T4-TCS (220 °C)	0.548 (0.541 ± 0.005)	1.31 (1.30 ± 0.10)	34.72 (34.47 ± 0.24)	0.25 (0.24 ± 0.01)

^aThe statistical values in parentheses are obtained from 10 cells.

■ DEVICE PERFORMANCE AND INTRINSIC STABILITY TESTING

The major goal of this study was to explore whether incorporating TCS units into the original PffBT-T4-OD polymer could increase the intrinsic morphological stability of the BHJ devices while retaining the device efficiency. As the final step of this study, BHJ solar cells made with polymer:PC₇₁BM were fabricated in an inverted structure according to previous literature.⁶ Details of device fabrication and characterization are included in Section 5 of the Supporting Information. Figure 6a presents the device efficiency vs TCS content before and after thermal cleavage (i.e., annealing the BHJ film at 220 °C for 30 min). Again, a larger film thickness reduction was observed in the BHJ after thermal annealing with increasing TCS content (Table S8). The OD reference polymer (i.e., 0% TCS in Figure 6a) without thermal annealing yields the highest PCE value of 9.17%, close to the expected efficiency for this polymer system.⁶ However, after the 220 °C annealing, device efficiencies plummeted to 2.10% with the largest loss in J_{sc} (Table S9 and Figure S21). On the other hand, the 100% TCS polymer, PffBT-T4-TCS, only offers very low efficiency numbers: 0.29% and 0.24% respectively for before and after thermal annealing at 220 °C. Similar results were reported earlier for a fully cleavable benzothiadiazole–terthiophene-based TCS polymer, which was attributed to poor aggregation of that polymer.³⁵ Overall, PffBT-T4-OD (i.e., 0% TCS) delivers the highest efficiency as expected; however, the morphology of its BHJ blend is rather fragile when subjected to high temperature, consistent with previous discoveries by Li et al.³⁹ By contrast, PffBT-T4-TCS (i.e., 100% TCS) is not able

to construct an effective charge transport channel due to lack of forming sufficient aggregation in its BHJ blend, resulting in the observed low efficiency; this nonideal morphology was not improved (and likely further exacerbated) after thermocleavage.

Pleasingly, the three copolymer (TCS50, -60 and, -70)-based devices show much better performance metrics than the PffBT-T4-TCS polymer (i.e., TCS100). Before thermocleavage, all three copolymers delivered PCEs around 3–4% (Table 4); after the 220 °C annealing to remove the alkyl chains, these numbers slightly decrease to 2.75, 3.16, and 2.71% for TCS50, TCS60, and TCS70 polymers, respectively. A closer look at the device characteristics (before and after thermocleavage) reveals that the open circuit voltage (V_{oc}) and fill factor (FF) are noticeably improved for the device after thermocleavage, yet the short circuit current (J_{sc}) is significantly reduced (by almost 50%). We tentatively ascribe these observed differences to morphological changes of the BHJ film after thermocleavage, which requires a detailed morphological study and device physics (out of the scope for this work). Nevertheless, these PCEs (~3%) represent the highest values to date for polymers having TCS used for BHJ solar cells.^{33–36}

Because the TCS60 copolymer demonstrates the highest efficiency in its device and best thermal stability in its neat polymer film, this polymer was chosen to compare with the reference polymer (PffBT-T4-OD) in BHJ devices for further thermal stability study (duration of 2 weeks at 100 °C) (Figure 6b). These tests were performed in an inert atmosphere in the dark to examine intrinsic degradation by heat only. For the reference polymer-based device, 34% of the initial efficiency was lost after 2 days and over 70% was lost after 2 weeks. By contrast, the TCS60-based device lost roughly 18% of the

initial efficiency after the initial 2 days (likely due to the burn-in loss) but only lost an additional 4% after 2 weeks. These results clearly demonstrate that applying TCS to modern push–pull low-band-gap polymer can significantly improve the device stability over high temperature (e.g., 100 °C).

CONCLUSIONS

The most important finding is that the strategy of partial cleavage of alkyl chains can also be applied to modern “push–pull” conjugated polymers to achieve significantly higher thermal stability of BHJ solar cells while retaining much of the efficiency achieved from the parent system. While PffBT-T4-OD (the parent system) can achieve close to 10% efficiency of its PSCs, over 70% of its original efficiency was lost after 2 weeks under our test conditions (100 °C, inert atmosphere). By contrast, the copolymer TCS60 could achieve a modest efficiency of 3.2% after thermally removing alkyl chains, but its PCE was retained at the ~80% level under the same testing conditions, and its BHJ morphology appeared to be extremely stable for an extended period of time. Together with our earlier results on applying partial cleavage to the P3HT system,²⁷ our new results indicate that this partial cleavage strategy could be generally applicable to other high-efficiency polymer-based BHJ systems.

Detailed thermal analysis revealed that extending the length of the cleavable alkyl chains can noticeably increase the cleavage temperature; furthermore, polymers with higher rigidity require higher temperature for cleaving alkyl chains, and the cleavage is slower when compared with more amorphous polymers. However, these factors do not have an impact on the activation energy of the thermocleavage because the mechanism of thermocleavage primarily concerns the functional groups employed (tertiary ester in our case).

Nevertheless, there are remaining questions that need further study. For example, what causes the relatively low efficiency of TCS60 (after thermocleavage)-based PSCs compared with the reference (PffBT-T4-OD)? Thermal treatment induced morphological change is certainly a serious concern. In fact, our previous work had discovered the strong impact on the morphology of TCS-containing polythiophenes.⁴⁶ Thus, methods to control temperature-dependent morphology and engineering solutions to avoid reductions in film quality should be further developed. On the other hand, if high-temperature annealing (e.g., 220 °C, 30 min) were the primary factor to account for the observed modest efficiency, we can design new methods to lower the temperature for removing alkyl chains. Increased efforts in these directions would further advance the TCS strategy where not only the thermal stability of the resulting optoelectronic device is enhanced but also the optoelectronic performance can be retained or even improved.

METHODS

General Methods. All chemicals were purchased from a commercial source (Sigma-Aldrich, Fisher, Acros, etc.) and used as received, except when specified. High-temperature size exclusion chromatography (HT-SEC) was performed relative to the polystyrene standards in hot 1,3,5-trichlorobenzene at 90 °C on a TOSOH EcoSEC high-temperature GPC system with an RI detector. ¹H nuclear magnetic resonance (NMR) measurements were recorded with Bruker DRX spectrometers (400 or 600 MHz). Absorption spectra were obtained with a Shimadzu UV-2600 spectrophotometer. IR spectra were taken on a Bruker Optics Hyperion 1000 with a Tensor 27. The film thicknesses were recorded with a profilometer

(Alpha-Step 200, Tencor Instruments). Differential scanning calorimetric measurements were performed on a TA Instruments Discovery DSC instrument at a heating and cooling rate of 10 °C/min. Thermal gravimetric analysis (TGA) was performed on a TA Instruments Q500 thermogravimetric analyzer under a nitrogen atmosphere. The thermomechanical behavior of the polymers was characterized using a TA Instruments DMA 850. The polymers were drop-cast onto a woven glass mesh that was then loaded into the DMA following a previously described process.³³

Device Fabrication. The PSCs were fabricated with a device structure of ITO/ZnO/PffBT-T4-based polymers:PC₇₁BM/MoO₃/Al, where ITO, ZnO, and MoO₃ refer to indium tin oxide, zinc oxide, and molybdenum oxide, respectively. Patterned ITO-coated glass substrates (size of 1.5 cm × 1.5 cm) were rinsed using detergent, acetone, and isopropanol for 15 min. The substrates were treated with ultraviolet-ozone plasma for 15 min. ZnO solution was spin-coated at 3500 rpm 60 s onto the ITO surface, followed by annealing at 200 °C for 1 h under air. Subsequently, ZnO-coated substrates were relocated to a glovebox filled with inert nitrogen gas. The solutions of the active layer (PffBT-T4-OD, PffBT-T4-TCS50, PffBT-T4-TCS60, or PffBT-T4-TCS70:PC₇₁BM) were prepared with a donor:acceptor ratio of 1:1.2 in CB::o-DCB (50:50) containing 3% v/v diiodooctane additive with total concentration of 22 mg mL⁻¹. In the case of the PffBT-T4-TCS100:PCBM solution, it was prepared with a concentration of 40 mg mL⁻¹. Before spin-coating, all solutions were stirred at 150 °C for 2 h. Note that all substrates were preheated on a hot plate at 120 °C. The solutions were spin-coated onto the ZnO layer with a thickness of ~200 nm. Next, the PffBT-T4-TCS-based films were treated with thermal annealing (220 °C, 30 min) for thermal cleavage. Finally, MoO₃ (thickness: 10 nm) and Al (thickness: 100 nm) were deposited under vacuum (<5.0 × 10⁻⁶ Pa). The active area of each sample was 0.068 cm².

ASSOCIATED CONTENT

Supporting Information

The Supporting Information is available free of charge at <https://pubs.acs.org/doi/10.1021/acs.chemmater.3c02181>.

Detailed synthetic procedures; basic information on P3ET, P3ET(C10), and PffBT-T4-TCSx polymers; ¹H NMR spectra; DMA scans; DSC thermograms; FT-IR; data for the stability test including UV-vis spectra and photos of films; and *J*–*V* curves and photovoltaic parameters for all devices ([PDF](#))

AUTHOR INFORMATION

Corresponding Author

Wei You – Department of Chemistry, University of North Carolina at Chapel Hill, Chapel Hill, North Carolina 27599, United States;  orcid.org/0000-0003-0354-1948; Email: wyou@unc.edu

Authors

Jordan Shanahan – Department of Chemistry, University of North Carolina at Chapel Hill, Chapel Hill, North Carolina 27599, United States

Jiyeon Oh – Department of Chemistry, University of North Carolina at Chapel Hill, Chapel Hill, North Carolina 27599, United States

Sung Yun Son – Department of Chemistry, Kwangwoon University, Seoul 01897, Korea;  orcid.org/0000-0003-1563-5474

Salma Siddika – Department of Mechanical and Aerospace Engineering, North Carolina State University, Raleigh, North Carolina 27695, United States

David Pendleton — *Department of Chemistry, University of North Carolina at Chapel Hill, Chapel Hill, North Carolina 27599, United States*

Brendan T. O'Connor — *Department of Mechanical and Aerospace Engineering, North Carolina State University, Raleigh, North Carolina 27695, United States*

Complete contact information is available at:
<https://pubs.acs.org/10.1021/acs.chemmater.3c02181>

Notes

The authors declare no competing financial interest.

ACKNOWLEDGMENTS

This work was financially supported by the National Science Foundation (NSF) under Award DMR-2210586 (for J.S., S.Y.S., D.P., and W.Y.) and ONR (N00014-20-1-2181, for J.O. and W.Y.). B.O. and S.S. acknowledge support from the NSF (Award CMMI-1554322). A Bruker NEO 600 MHz NMR spectrometer was supported by the National Science Foundation under Grant CHE-1828183. The authors thank Dr Marc A. ter Horst from the University of North Carolina's Department of Chemistry NMR Core Laboratory for the use of the NMR spectrometers and Dr. Carrie Donley for IR characterization.

REFERENCES

- (1) Yu, G.; Gao, J.; Hummelen, J. C.; Wudl, F.; Heeger, A. J. Polymer Photovoltaic Cells: Enhanced Efficiencies via a Network of Internal Donor-Acceptor Heterojunctions. *Science* **1995**, *270* (5243), 1789–1791.
- (2) Liu, Y.; Li, B.; Ma, C.; Huang, F.; Feng, G.; Chen, H.; Zou, Y.; Chen, Y.; Li, Y.; Chen, Y.; Tang, Z. Recent Progress in Organic Solar Cells (Part I Material Science). *Sci. China Chem.* **2022**, *64*, 224–268.
- (3) Zhang, G.; Lin, F. R.; Qi, F.; Heumüller, T.; Distler, A.; Egelhaaf, H.; Li, N.; Chow, P. C. Y.; Brabec, C. J.; Jen, K.; Yip, H. The Renewed Prospects for Organic Photovoltaics The Renewed Prospects for Organic Photovoltaics. *Chem. Rev.* **2022**, *122* (18), 14180–14274.
- (4) Zhou, H.; Yang, L.; You, W. Rational Design of High Performance Conjugated Polymers for Organic Solar Cells. *Macromolecules* **2012**, *45* (2), 607–632.
- (5) Zhou, H.; Yang, L.; Stoneking, S.; You, W. A Weak Donor-Strong Acceptor Strategy to Design Ideal Polymers for Organic Solar Cells. *ACS Appl. Mater. Interfaces* **2010**, *2* (5), 1377–1383.
- (6) Liu, Y.; Zhao, J.; Li, Z.; Mu, C.; Ma, W.; Hu, H.; Jiang, K.; Lin, H.; Ade, H.; Yan, H. Aggregation and Morphology Control Enables Multiple Cases of High-Efficiency Polymer Solar Cells. *Nat. Commun.* **2014**, *5* (9), 5293.
- (7) Zhan, L.; Li, S.; Li, Y.; Sun, R.; Min, J.; Chen, Y.; Fang, J.; Ma, C.; Zhou, G.; Zhu, H.; Zuo, L.; Qiu, H.; Yin, S.; Chen, H. Manipulating Charge Transfer and Transport via Intermediary Electron Acceptor Channels Enables 19. 3% Efficiency Organic Photovoltaics. *Adv. Energy Mater.* **2022**, *12*, 2201076.
- (8) Zhang, G.; Zhao, J.; Chow, P. C. Y.; Jiang, K.; Zhang, J.; Zhu, Z.; Zhang, J.; Huang, F.; Yan, H. Nonfullerene Acceptor Molecules for Bulk Heterojunction Organic Solar Cells. *Chem. Rev.* **2018**, *118* (7), 3447–3507.
- (9) Mateker, W. R.; McGehee, M. D. Progress in Understanding Degradation Mechanisms and Improving Stability in Organic Photovoltaics. *Adv. Mater.* **2017**, *29* (10), 1603940.
- (10) Xu, X.; Li, D.; Yuan, J.; Zhou, Y.; Zou, Y. Recent Advances in Stability If Organic Solar Cells. *EnergyChem* **2021**, *3* (1), 100046.
- (11) Wang, Y.; Lee, J.; Hou, X.; Labanti, C.; Yan, J.; Mazzolini, E.; Parhar, A.; Nelson, J.; Kim, J. S.; Li, Z. Recent Progress and Challenges toward Highly Stable Nonfullerene Acceptor-Based Organic Solar Cells. *Adv. Energy Mater.* **2021**, *11*, 2003002.
- (12) Ghasemi, M.; Balar, N.; Peng, Z.; Hu, H.; Qin, Y.; Kim, T.; Rech, J. J.; Bidwell, M.; Mask, W.; McCulloch, I.; You, W.; Amassian, A.; Risko, C.; O'Connor, B. T.; Ade, H. A Molecular Interaction-Diffusion Framework for Predicting Organic Solar Cell Stability. *Nat. Mater.* **2021**, *20*, 525–532.
- (13) Xie, R.; Weisen, A. R.; Lee, Y.; Aplan, M. A.; Fenton, A. M.; Masucci, A. E.; Kempe, F.; Sommer, M.; Pester, C. W.; Colby, R. H.; Gomez, E. D. Glass Transition Temperature from the Chemical Structure of Conjugated Polymers. *Nat. Commun.* **2020**, *11* (1), 893.
- (14) Qian, Z.; Cao, Z.; Galuska, L.; Zhang, S.; Xu, J.; Gu, X. Glass Transition Phenomenon for Conjugated Polymers. *Macromol. Chem. Phys.* **2019**, *220* (11), 1900062.
- (15) Balar, N.; Rech, J. J.; Siddika, S.; Song, R.; Schrickx, H. M.; Sheikh, N.; Ye, L.; Megret Bonilla, A.; Awartani, O.; Ade, H.; You, W.; O'Connor, B. T. Resolving the Molecular Origin of Mechanical Relaxations in Donor–Acceptor Polymer Semiconductors. *Adv. Funct. Mater.* **2022**, *32* (4), 2105597.
- (16) Gevorgyan, S. A.; Krebs, F. C. Bulk Heterojunctions Based on Native Polythiophene. *Chem. Mater.* **2008**, *20*, 4386–4390.
- (17) Krebs, F. C. Design and applications of polymer solar cells with lifetimes longer than 10000 h. *Proc. SPIE, Organic Photovoltaics VI*, **2005**, 5938, 59380Y.
- (18) Nielsen, C. B.; Sohn, E. H.; Cho, D. J.; Schroeder, B. C.; Smith, J.; Lee, M.; Anthopoulos, T. D.; Song, K.; McCulloch, I. Improved Field-Effect Transistor Performance of a Benzotriithiophene Polymer through Ketal Cleavage in the Solid State. *ACS Appl. Mater. Interfaces* **2013**, *5* (5), 1806–1810.
- (19) Ponder, J. F.; Gregory, S. A.; Atassi, A.; Menon, A. K.; Lang, A. W.; Savagian, L. R.; Reynolds, J. R.; Yee, S. K. Significant Enhancement of the Electrical Conductivity of Conjugated Polymers by Post-Processing Side Chain Removal. *J. Am. Chem. Soc.* **2022**, *144* (3), 1351–1360.
- (20) Hillebrandt, S.; Adermann, T.; Alt, M.; Schinke, J.; Glaser, T.; Mankel, E.; Hernandez-Sosa, G.; Jaegermann, W.; Lemmer, U.; Pucci, A.; Kowalsky, W.; Müllen, K.; Lovrincic, R.; Hamburger, M. Naphthalene Tetracarboxydiimide-Based n-Type Polymers with Removable Solubility via Thermally Cleavable Side Chains. *ACS Appl. Mater. Interfaces* **2016**, *8* (7), 4940–4945.
- (21) Ngai, J. H. L.; Gao, X.; Kumar, P.; Polena, J.; Li, Y. A Highly Stable Diketopyrrolopyrrole (DPP) Polymer for Chemiresistive Sensors. *Adv. Electron. Mater.* **2021**, *7* (3), 202000935.
- (22) Son, S. Y.; Lee, G.; Wang, H.; Samson, S.; Wei, Q.; Zhu, Y.; You, W. Integrating Charge Mobility, Stability and Stretchability within Conjugated Polymer Films for Stretchable Multifunctional Sensors. *Nat. Commun.* **2022**, *13* (1), 2739.
- (23) Freudenberg, J.; Jänsch, D.; Hinkel, F.; Bunz, U. H. F. Immobilization Strategies for Organic Semiconducting Conjugated Polymers. *Chem. Rev.* **2018**, *118*, 5598.
- (24) Schmatz, B.; Yuan, Z.; Lang, A. W.; Hernandez, J. L.; Reichmanis, E.; Reynolds, J. R. Aqueous Processing for Printed Organic Electronics: Conjugated Polymers with Multistage Cleavable Side Chains. *ACS Cent. Sci.* **2017**, *3* (9), 961–967.
- (25) Smith, Z. C.; Meyer, D. M.; Simon, M. G.; Staii, C.; Shukla, D.; Thomas, S. W. Thiophene-Based Conjugated Polymers with Photolabile Solubilizing Side Chains. *Macromolecules* **2015**, *48* (4), 959–966.
- (26) Bundgaard, E.; Hagemann, O.; Bjerring, M.; Nielsen, N. C.; Andreasen, J. W.; Andreasen, B.; Krebs, F. C. Removal of Solubilizing Side Chains at Low Temperature: A New Route to Native Poly(Thiophene). *Macromolecules* **2012**, *45* (8), 3644–3646.
- (27) Son, S. Y.; Samson, S.; Siddika, S.; O'Connor, B. T.; You, W. Thermocleavage of Partial Side Chains in Polythiophenes Offers Appreciable Photovoltaic Efficiency and Significant Morphological Stability. *Chem. Mater.* **2021**, *33* (12), 4745–4756.
- (28) Qin, Y.; Balar, N.; Peng, Z.; Gadisa, A.; Angunawela, I.; Bagui, A.; Kashani, S.; Hou, J.; Ade, H. The Performance-Stability Conundrum of BTP-Based Organic Solar Cells. *Joule* **2021**, *5* (8), 2129–2147.

(29) Sai, N.; Leung, K.; Zádor, J.; Henkelman, G. First Principles Study of Photo-Oxidation Degradation Mechanisms in P3HT for Organic Solar Cells. *Phys. Chem. Chem. Phys.* **2014**, *16* (17), 8092–8099.

(30) Petersen, M. H.; Gevorgyan, S. A.; Krebs, F. C. Thermocleavable Low Band Gap Polymers and Solar Cells Therefrom with Remarkable Stability toward Oxygen. *Macromolecules* **2008**, *41* (23), 8986–8994.

(31) Manceau, M.; Helgesen, M.; Krebs, F. C. Thermo-Cleavable Polymers: Materials with Enhanced Photochemical Stability. *Polym. Degrad. Stab.* **2010**, *95* (12), 2666–2669.

(32) Aoyama, Y.; Yamanari, T.; Kourumura, N.; Tachikawa, H.; Nagai, M.; Yoshida, Y. Photo-Induced Oxidation of Polythiophene Derivatives: Dependence on Side Chain Structure. *Polym. Degrad. Stab.* **2013**, *98* (4), 899–903.

(33) Liu, J.; Kadnikova, E. N.; Liu, Y.; McGehee, M. D.; Fréchet, J. M. J. Polythiophene Containing Thermally Removable Solubilizing Groups Enhances the Interface and the Performance of Polymer-Titania Hybrid Solar Cells. *J. Am. Chem. Soc.* **2004**, *126* (31), 9486–9487.

(34) Helgesen, M.; Krebs, F. C. Photovoltaic Performance of Polymers Based on Dithienylthienopyrazines Bearing Thermocleavable Benzoate Esters. *Macromolecules* **2010**, *43*, 1253–1260.

(35) Helgesen, M.; Gevorgyan, S. A.; Krebs, F. C.; Janssen, A. J. Substituted 2, 1, 3-Benzothiadiazole- And Thiophene-Based Polymers for Solar Cells - Introducing a New Thermocleavable Precursor. *Chem. Mater.* **2009**, *21*, 4669–4675.

(36) Liu, C.; Dong, S.; Cai, P.; Liu, P.; Liu, S.; Chen, J.; Liu, F.; Ying, L.; Russell, T. P.; Huang, F.; Cao, Y. Donor-Acceptor Copolymers Based on Thermally Cleavable Indigo, Isoindigo, and DPP Units: Synthesis, Field Effect Transistors, and Polymer Solar Cells. *ACS Appl. Mater. Interfaces* **2015**, *7* (17), 9038–9051.

(37) Hu, H.; Jiang, K.; Yang, G.; Liu, J.; Li, Z.; Lin, H.; Liu, Y.; Zhao, J.; Zhang, J.; Huang, F.; Qu, Y.; Ma, W.; Yan, H. Terthiophene-Based D–A Polymer with an Asymmetric Arrangement of Alkyl Chains That Enables Efficient Polymer Solar Cells. *J. Am. Chem. Soc.* **2015**, *137* (44), 14149–14157.

(38) Ghasemi, M.; Hu, H.; Peng, Z.; Rech, J. J.; Angunawela, I.; Carpenter, J. H.; Stuard, S. J.; Wadsworth, A.; McCulloch, I.; You, W.; Ade, H. Delineation of Thermodynamic and Kinetic Factors That Control Stability in Non-Fullerene Organic Solar Cells. *Joule* **2019**, *3* (5), 1328–1348.

(39) Li, N.; Perea, J. D.; Kassar, T.; Richter, M.; Heumueller, T.; Matt, G. J.; Hou, Y.; Güldal, N. S.; Chen, H.; Chen, S.; Langner, S.; Berlinghof, M.; Unruh, T.; Brabec, C. J. Abnormal Strong Burn-in Degradation of Highly Efficient Polymer Solar Cells Caused by Spinodal Donor-Acceptor Demixing. *Nat. Commun.* **2017**, *8*, 14541.

(40) Flynn, J. H.; Wall, L. A. General Treatment of the Thermogravimetry of Polymers. *J. Res. Natl. Bur. Stand.* (1934). **1966**, *70* (6), 487–523.

(41) Van Speybroeck, V.; Waroquier, M.; Martelé, Y.; Schacht, E. Ab Initio and Experimental Study on Thermally Degradable Polycarbonates: Effect of Substituents on the Reaction Rates. *J. Am. Chem. Soc.* **2001**, *123* (43), 10650–10657.

(42) Van Speybroeck, V.; Martelé, Y.; Schacht, E.; Waroquier, M. Ab Initio Studies of Thermal Syn-Elimination Reactions in Carbonates: Effect of Structure on Reactivity. *J. Phys. Chem. A* **2002**, *106* (51), 12370–12375.

(43) Kuhn, M.; Ludwig, J.; Marszalek, T.; Adermann, T.; Pisula, W.; Müllen, K.; Colsmann, A.; Hamburger, M. Tertiary Carbonate Side Chains: Easily Tunable Thermo-Labile Breaking Points for Controlling the Solubility of Conjugated Polymers. *Chem. Mater.* **2015**, *27* (7), 2678–2686.

(44) Helgesen, M. Thermocleavable π -Conjugated Polymers - Synthesis and Photovoltaic Applications. PhD Dissertation, Riso National Laboratory, Technical University of Denmark, 2009.

(45) Pomerantz, M.; Amarasekara, A. S.; Dias, H. V. R. Synthesis and Solid-State Structures of Dimethyl 2, 2' -Bithiophenedicarboxylates. *J. Org. Chem.* **2002**, *67* (20), 6931–6937.

(46) Zhao, H.; Shanahan, J. J.; Samson, S.; Li, Z.; Ma, G.; Prine, N.; Galuska, L.; Wang, Y.; Xia, W.; You, W.; Gu, X. Manipulating Conjugated Polymer Backbone Dynamics through Controlled Thermal Cleavage of Alkyl Side Chains. *Macromol. Rapid Commun.* **2022**, *43*, 202200533.

□ Recommended by ACS

Polymer Acceptor with Hydrogen-Bonding Functionality for Efficient and Mechanically Robust Ternary Organic Solar Cells

Qingpei Wan, Barry C. Thompson, *et al.*

DECEMBER 14, 2023

CHEMISTRY OF MATERIALS

READ 

Fused Benzotriazole A-Unit Constructs a D- π -A Polymer Donor for Efficient Organic Photovoltaics

Zehua He, Erjun Zhou, *et al.*

JULY 28, 2023

ACS MACRO LETTERS

READ 

Incorporating a Nonfused Electron Acceptor into Double-Cable Conjugated Polymers for Single-Component Organic Solar Cells with a Photo Response up to 900 nm

Xiaojing Liu, Weiwei Li, *et al.*

OCTOBER 25, 2023

MACROMOLECULES

READ 

Direct C–H Arylation-Derived Donor Polymers Afford PCEs over 10% for Organic Solar Cells

Ling-Jun Yang, Shi-Yong Liu, *et al.*

AUGUST 23, 2023

ACS APPLIED POLYMER MATERIALS

READ 

Get More Suggestions >